ORIGINAL ARTICLE

Conversion of murine antibodies to human antibodies and their optimization for ovarian cancer therapy targeted to the folate receptor

Mariangela Figini · Franck Martin · Renata Ferri · Elena Luison · Elena Ripamonti · Alberto Zacchetti · Mimosa Mortarino · Vito Di Cioccio · Giovanni Maurizi · Marcello Allegretti · Silvana Canevari

Abstract We previously developed murine and chimeric antibodies against a specific epithelial ovarian carcinoma (EOC) marker, named folate receptor (FR), and promising results were obtained in phase II trials. More recently, we successfully generated a completely human *Fab* fragment, C4, by conversion of one of the murine anti-FR antibodies to human antibody using phage display and guided selection. However, subsequent efforts to obtain C4 in a dimer format, which seems especially desirable for EOC locoregional treatment, resulted in a highly heterogeneous product upon natural dimerization and in a very poor production yield upon chemical dimerization by a non-hydrolyzable linker to a di-*Fab*-maleimide (DFM). We therefore designed, constructed and characterized a large *Fab* dual combinatorial human antibody phage display library obtained from EOC patients and potentially biased toward an anti-tumor response in an effort to obtain new anti-FR human antibodies suitable for therapy. Using this library and guiding the selection on FR-expressing cells with murine/human antibody chains, we generated four new human anti-FR antibody (AFRA) *Fab* fragments, one of which was genetically and chemically manipulated to obtain a chemical dimer, designated AFRA-DFM5.3, with high yield production and the capability for purification scaled-up to clinical grade. Overall affinity of AFRA-DFM5.3 was in the 2-digit nanomolar range, and immunohistochemistry indicated that the reagent recognized the FR expressed on EOC samples. ^{131}I-AFRA-DFM5.3 showed high immunoreactivity, in vitro stability and integrity, and specifically accumulated only in FR-expressing tumors in subcutaneous preclinical in vivo models. Overall, our studies demonstrate the successful conversion of murine to completely human anti-FR antibodies through the combined use of antibody phage display libraries biased toward an anti-tumor response, guided selection and chain shuffling, and point to the suitability of AFRA5.3 for future clinical application in ovarian cancer.

Keywords Antibody fragment · Phage display · Folate receptor · Ovarian cancer · Chemical dimerization

M. Figini · R. Ferri · E. Luison · E. Ripamonti · A. Zacchetti · M. Mortarino · S. Canevari (✉)
Unit of Molecular Therapies,
Department of Experimental Oncology and Laboratories,
Fondazione IRCCS Istituto Nazionale dei Tumori,
Via Venezian 1, 20133 Milan, Italy
e-mail: silvana.canevari@istitutotumori.mi.it

M. Figini
e-mail: mariangela.figini@istitutotumori.mi.it

F. Martin · V. Di Cioccio · G. Maurizi · M. Allegretti
Dompé Pharma, L'Aquila, Italy

Abbreviation

EOC	Epithelial ovarian carcinoma
FR	Folate receptor
DFM	Di-*Fab*-maleimide
AFRA	Anti-FR antibody
mAb(s)	Monoclonal antibody/ies
PBMC	Peripheral blood mononuclear cells
chi	Chimeric
TCEP	Tris (2-carboxyethyl) phosphine hydrochloride
BMOE	Bismaleimidoethane
RP-HPLC	Reverse phase-high performance liquid chromatography
SDS-PAGE	Sodium dodecyl sulfate-polyacrylamide gel electrophoresis
IC_{50}	Concentration inhibiting 50% of binding
s.c.	Subcutaneous

i.v. Intravenous

%ID/g Percentage of the injected dose per unit mass of organ

Introduction

Targeted therapy is a major area of interest for many solid tumors, and monoclonal antibodies (mAbs) are among the most promising vehicles for targeting the cytotoxic effects of drugs or radionuclides to the tumor site. Targeted therapy requires the identification of suitable target molecules that are sufficiently overexpressed and tumor-specific. The 38–40 kDa GPI-anchored molecule [3], overexpressed on ovarian cancer cells [29] and identified by screening of a cDNA library as the alpha isoform of the folate receptor (FR) [13], is one of the most promising targets for ovarian carcinoma therapy. The FR, a member of the family of homologous proteins that bind folic acid with high affinity [37] and overexpressed on 90% of epithelial ovarian carcinomas (EOC), can be blocked at the membrane level using an intracellular antibody to partially revert the tumor phenotype [17]. This result, along with evidence that FR expression is stable or even up-modulated during ovarian cancer progression and acquisition of drug resistance [32, 38] and that the molecule is localized in membrane microdomains and not internalized under physiologic conditions [8, 9, 27], clearly point to FR as an appropriate target for immunotherapy with mAb-based reagents.

Monoclonal antibodies and their recombinant derivatives have proven to be well-tolerated, disease-specific therapeutic tools able to deliver clinical benefit to patients with diseases caused by infectious agents, autoimmunity and cancer [34]. We previously developed a panel of anti-ovary carcinoma murine mAbs subsequently shown to recognize different epitopes of the FR. Two of these mAbs, MOV18 (IgG1κ) and MOV19 (IgG2aκ), bound to ovarian tumor cells with high affinity (K_A range of 10^8–10^9 M^{-1} [29]) and were further exploited for therapeutic approaches. Encouraging results were obtained in two clinical phase II studies in which we used a murine anti-FR mAb, delivered intraperitoneally, to target ^{131}I [15] or to recruit the cytotoxicity of activated autologous T cells [6] to EOC.

A major limitation in clinical studies with murine reagents is the resulting human anti-mouse antibody response [30, 31, 33]. To overcome this problem, we initially generated mouse-human chimeras of these mAbs [12] and more recently, produced completely human antibody *Fab* fragments against FR using phage display and epitope imprinting selection [18], to isolate antibody with the same specificity as a preexisting antibody by guided selection.

Besides the immunogenicity of mAb, their structure, size and affinity also represent potential limitations to efficacy in treating solid tumors, since several factors including physical (interstitial pressure) and molecular (tumor microenvironment composition) barriers [21] have been demonstrated to hinder the penetration of antibodies into tumors. Indeed, molecular and chemical manipulations of antibody size and affinity have greatly enhanced tumor uptake of mAbs [7].

The particular localization of EOC tumors has made locoregional treatment with mAbs promising [6, 15, 28]. We speculated that a human antibody fragment in a dimer format might be the reagent of choice for such treatment, since the relatively small size of the fragment should favor tumor penetration, the dimer format might stabilize binding to the target antigen, and its human origin should limit the immunogenic reactions. Our efforts to improve the characteristics of C4 *Fab* by dimerization, which as a monomer exhibited good specificity and an estimated K_{aff} of 200 nM based on Scatchard analysis on entire EOC cells [19], have been hampered by a very poor production yield, limiting its exploitation in the clinical setting. Thus, we turned to the use of a large "*Fab* dual combinatorial human antibody phage display library" (DCL) obtained from patients with a previous history of EOC, combined with epitope imprinting selection methodology [18], to select a promising candidate subsequently optimized in a dimer format by molecular and chemical modification.

Materials and methods

Library construction and cloning

The procedures used for library construction and cloning were essential as described [18]. Peripheral blood mononuclear cells (PBMC) from four women with a clinical history of ovarian carcinoma and a disease-free status for several years after first-line treatment were the source of the variable regions of these libraries. Three of the women had carcinoma of the serous histotype, diagnosed at stage III or IV of disease; the fourth patient had ovarian carcinoma of the endometrioid histotype, diagnosed at stage III. PBMC (2.0–5.0 × 10^7) were separated by Ficoll gradient and used for library preparation.

All repertoires were generated by reverse transcription and PCR amplification of mRNA. Each chain family was separately amplified by appropriate primer pairs to compensate specific PCR bias introduced by different primers annealing temperature [18].

For display on the surface of phage fused with pIII, the heavy chain repertoire (VH) was cloned in the phage vector already containing the human CH1 (fdDOG-VH-Cγ1); the light chain repertoire was cloned in the phagemid vector pHEN1 (pHENCLLib [18]).

Cell lines and antibodies

The following human tumor cell lines were used: ovarian carcinomas IGROV1 (a gift from Dr. J. Bénard, Institute Gustave Roussy, Villejuif, France), OVCAR3 and SKOV3 [from the American Type Culture Collection (ATCC)], OAW42 (kindly provided by Dr. A. Ullrich, Max-Planck Institute of Biochemistry, Martinsried, Germany), and OVCA432 (kindly provided by Dr. R. Knapp, Dana Farber Institute, Boston, MA); melanoma Mewo (kindly provided by the late Dr. J. Fogh); epidermoid carcinoma A431 (from ATCC) and A431FR and A431Mock epidermoid carcinoma cells transfected with FR or with empty vector, respectively, derived in our laboratory as described [11]. Cell lines were grown in RPMI-1640 medium except for OAW42, which was maintained in MEM. Both media were supplemented with 10% FCS and 2 mM glutamine, and in the case of stably transfected cells, with G418 at 800 µg/ml (Gibco). Cells were maintained in a 5% CO_2 humidified atmosphere at 37°C and routinely tested for mycoplasma contamination. Only cell preparations consistently found negative were used.

Hybridomas\trasfectomas producing the murine mAbs MOV18 (IgG_1) and MOV19 (IgG_{2a}) and the chimeric mAb chiMOV19 (IgG_1) directed to FR [13, 29], and murine mAb 9E10 (IgG_1), directed to a myc sequence [18], were maintained in culture for antibody production and were affinity-purified from culture supernatants on proteinA/proteinG (High Trap Pharmacia Biotech) according to isotype. $F(ab)_2$ from chiMOV19 were prepared using the Immuno-Pure $F(ab)_2$ preparation kit (Pierce).

Guided selection

Light chain gene cloning of murine mAb, preparation of phage libraries displaying hybrid mouse/human *Fab* fragments, selection of FR-binding clones, cloning of the selected human VHCH1 into pHEN1-VLlib (an equimolar mixture of pHEN1 containing a pre-cloned repertoire of human kappa and lambda chain genes), and preparation of phages are described in detail elsewhere [19].

Selection and screening

The first screening was performed by phage-ELISA as positive binding on a monolayer of A431FR cells and as negative binding on A431Mock cells essentially as described [19]. Subsequently phages were selected on OVCAR3 or on A431FR cells.

Subcloning, expression and purification

To facilitate purification, the selected human *Fab* genes were subcloned into the expression vector pUC119SfiI/NotIHismyc [18], which results in the addition of a hexa-histidine tag at the C-terminal end of the *Fab* gene. A small amount of purified *Fab*s was produced at laboratory scale essentially as described [19].

Large scale expression and purification

The genes coding for the heavy and light chains of selected AFRA fragments were cloned in frame with leader sequences in order to address the fragment synthesis to the *Escherichia coli* periplasmic compartment; the expression vector was transformed in *E. coli* and fed batch cultures were run at high cell density (Chemap fermentor).

At the end of the fermentation the AFRA antibody fragments were recovered from culture supernatant (100 mg/l) and purified by three following chromatographic steps. The fragments were obtained in high purity (>99.9%) by reverse phase-high performance liquid chromatography (RP-HPLC) analysis (VYDAC 219TP54 di-Phenyl column, 250 mm × 4.6 mm), and the primary structure was confirmed by electrospray mass analysis (ThermoFinnigan DECA XP Plus).

Genetic modification of the N- and C-termini of C4-MOV19 mimicking heavy chain

To modify the DNA triplet codon of glutamine corresponding to the N terminus of the C4 and AFRA 5 heavy chain a site directed mutagenesis was performed. For this the Q1N mutation has been inserted during PCR amplification of the *Fab* heavy chain. Mutation was confirmed by sequencing the whole expression cassette. The penta-peptide DKTSC, corresponding to the natural hinge sequence of the gamma 1 human family, was added to the C-terminus of the C4 and AFRA 5 heavy chain. Following these genetic modifications the final *Fab* fragments were named AFRA4 and AFRA5.3, respectively.

AFRA antibody fragment dimerization

Natural dimerization

After monomer purification and to reduce the heavy chain carboxy terminal cysteine residue, naturally blocked by glutathione during fermentation, AFRA 4 and AFRA 5.3 fragments were incubated with Tris (2-carboxyethyl) phosphine hydrochloride (TCEP) at a 70 TCEP/*Fab'* molar ratio for 5 h at room temperature without mixing.

TCEP was removed by HiPrep Desalting chromatography 26/10 (GE Healthcare) previously equilibrated in MES 40 mM pH 6.0 and pH was further adjusted to 8, condition at which disulfide bond formation is known to be chemically favoured. Natural dimers were separated from the

reaction mixture by gel filtration chromatography on a Sephacryl S-100 HR XK50/800 column (GE Healthcare) where they were resolved as a unique peak.

Chemical dimerization

The chemical dimer DFM was prepared using the bifunctional linker bismaleimidoethane (BMOE) according to a described procedure [10]. Briefly, the heavy chain C-terminal cysteine residue was reduced as above described and TCEP was removed by HiPrep Desalting chromatography 26/10 previously equilibrated in MES 40 mM, pH 6.0. Protein was concentrated to 8 mg/ml and incubated with gentle stirring at room temperature for 2.5 h to allow the intramolecular disulfide bond formation. The reaction kinetics was monitored by RP-HPLC analysis (VYDAC Diphenyl 219TP54, 250 mm × 4.6 mm). BMOE linker (Sigma) was then added to the protein solution (1 mg/ml in DMSO) in a molar ratio of 0.35 linker/protein and reaction mixture incubated for 16 h at room temperature with gentle stirring. To remove natural $F(ab')_2$, the reaction mixture was again reduced at a TCEP/Fab' molar ratio of 70 for 3.5 h at room temperature. DFM was purified on a HiPrep Sephacryl S-100 HR column previously equilibrated with 40 mM MES, pH 6.0.

Characterization of reagents

Biochemical characterization

Purified proteins were quantified by the Bradford method and analyzed for purity and integrity by: (a) electrophoresis in sodium dodecyl sulfate-polyacrylamide gel electrophoresis (SDS-PAGE) in homogeneous 12.5% polyacrylamide gels using a Mini-Protean II electrophoresis System (Bio-Rad); (b) gel filtration chromatography (Sephacryl S-100 HR XK50/800 column) in physiologic conditions; (c) RP-HPLC analysis (VYDAC Diphenyl 219TP54 column, 250 mm × 4.6 mm).

BIAcore analysis

Kinetic analysis was performed by surface plasmon resonance with BIAcore equipment (Pharmacia). Soluble recombinant human FR (produced in the baculovirus expression system) was covalently bound to a CM5 sensor chip using the amine coupling kit (GE Healthcare) at an antigen concentration of 40 μg/ml in 10 mM sodium acetate, pH 4.8, yielding a surface of 280 RU. Residual activated groups were blocked by injection of 1.0 M ethanolamine, pH 8.5. Several concentrations of human antibody fragments were used to determine the binding kinetics, and the respective affinities were deduced from the binding curves.

The apparent kinetic dissociation rate constants (K_D) were calculated using the Wizard program under saturating conditions of antibody fragment from 200 to 3,125 nM, with a buffer flow rate of 50 μl/min. Dissociation was allowed to proceed for at least 30 min. Residual antibody fragment bound to the sensor chip was detached using 100 mM glycine buffer, pH 2.7.

ELISA and FACS binding evaluation

The binding activity and specificity of purified antibody/*Fab*/DFM was evaluated on fixed and live cells by ELISA and FACS, respectively, using techniques and reagents previously described [19].

Immunohistochemistry

Ovarian cancer samples were collected during surgical procedures from EOC patients undergoing debulking surgery at Fondazione IRCCS Istituto Nazionale dei Tumori. Tumor samples were obtained with Institutional Review Board approval from patients at the first diagnosis and not previously treated with chemotherapeutic regimens. All patients gave informed consent to use leftover biologic material for investigational purposes. Frozen sections, 5 mm thick, were cut, dried and fixed in cold acetone for 5 min. Excess acetone was removed by washing slides in PBS (pH 7.4) and air-drying. AFRA-DFM5.3 and murine MOV19 were biotinylated using the biotin *N*-Hydroxy-succinimide ester (10× molar excess compared to the mAb). After blocking endogenous biotin with avidin-biotin blocking solution (avidin solution + PBS + biotin solution, each step for 15 min), slides were pre-incubated with normal goat serum (Vector Laboratories, Burlingame, CA) at room temperature for 15 min and further incubated with biotinylated antibodies overnight at 4°C in a humidified chamber followed by endogenous peroxidase blocking at room temperature for 30 min with 0.5% H_2O_2 in PBS. All slides were incubated with avidin-biotin-complex (Vectastain ABC Kit, Vector Laboratories) for an additional 30 min at room temperature. After each incubation step, sections were washed three times for 5 min each with PBS. Diaminobenzidine tablets (Sigma) appropriately diluted in PBS and left to react for 5 min in the dark served as chromogen. After counterstaining with hematoxylin, sections were washed in tap water, dehydrated and mounted with coverslips.

Radiolabeling

AFRA-DFM5.3 was radiolabeled with [131]I (GE Healthcare) using Iodogen-precoated iodination tubes (Pierce) by the Chizzonite method, essentially as described by the manu-

facturer using pyrogen-free, clinical grade reagents. The efficiency of radiolabeling was $86 \pm 1.5\%$ (mean $\pm$ SD, four experiments), and the radiolabeled dimer was purified by chromatography on disposable PD-10 desalting columns equilibrated and eluted with 100 mM sodium phosphate, pH 7.4, 150 mM NaCl and 2% HSA. Products were filtered through a sterile 0.22-μm membrane. Sterility and pyrogen contamination were evaluated as described [11].

Immunoreactivity was assayed on 1×10^7 A431FR or OVCAR3 cells incubated with trace amounts of radiolabeled dimer in 50 μl of 0.03% bovine serum albumin in PBS for 3 h at room temperature with gentle rotation. Nonspecific binding was evaluated on Mewo or A431Mock cells. Cells were washed three times with cold medium and assessed for radioactivity in a gamma-counter. Radiolabeled dimers were examined by SDS-PAGE in homogeneous 12.5% polyacrylamide gels in non-reducing conditions using the Phast System (Amersham Pharmacia Biotech) and visualized by autoradiography.

Radiolabeled dimers were used to evaluate the epitope similarity by competition assay. Briefly FR-expressing cells (5×10^4) were incubated for 3 h on ice with a fixed amount of ^{131}I-AFRA-DFM5.3 (final concentration 22 nM) mixed with serial dilutions of purified AFRA-DFM5.3, chiMOV18, chiMOV19 and $(Fab)_2$ chiMOV19 (starting from 3 μM) or buffer alone. After three washes with cold buffer, cell-bound radioactivity was measured directly in a gamma-counter. The concentration inhibiting 50% of ^{131}I-AFRA-DFM5.3 binding (IC_{50}) was extrapolated from titration curves.

For evaluation of stability in serum, ^{131}I-AFRA-DFM5.3 at 0.5-1 μM (final concentration) was diluted in 500 μl fresh human serum and incubated at 4 or 37°C for 24 h. SDS-PAGE was used to control for any potential degradation, and direct binding on fixed FR-expressing cells was used to assess functionality.

Preclinical in vivo experiments

All protocols were approved by the Ethics Committee for Animal Experimentation of the National Cancer Institute of Milan and carried out according to institutional guidelines [1]. Female CD1 *nu/nu* mice (athymic) were obtained at 5–6 weeks of age from Charles River Laboratories (Calco, Italy). After 1 week of acclimatization, mice were used for pharmacokinetics and/or biodistribution analyzes.

Animals were xenografted subcutaneously (s.c.) with 3.5×10^6 A431FR or A431Mock cells in 0.1 ml of 0.9% NaCl. An initial experiment was performed in which mice were injected with unlabeled AFRA-DFM5.3 (200 μg/mouse) 3 weeks after cell injection and tumors were harvested 12 or 24 h following dimer injection (three mice per group). In subsequent experiments, mice were injected with

tumor cells and after about 2 weeks, when average tumor volume reached 0.4–0.5 cm^3, randomly divided into groups and injected intravenously (i.v.) in the lateral tail vein with 0.3 ml of 0.9% NaCl in the presence or absence of ^{131}I-AFRA-DFM5.3 fragments (1–1.5 MBq/mouse). Three independent experiments (four mice per group) were performed. Blood was collected for pharmacokinetics analysis at the following time points: 10 and 30 min, 1, 3, 6, 15, 24, 48 h. The blood pharmacokinetics of ^{131}I-AFRA-DFM5.3 was calculated using a mono-exponential function: $y(t) = C_{max} \times e^{-\lambda t}$, where C_{max} is the blood concentration at $t = 0$, to fit the decay-corrected activity measurements in blood and used to derive the blood global half-life ($t_{\frac{1}{2}}$). Except for the first two time points, mice were sacrificed for biodistribution and tumor localization assessment. After dissection, tumors and other tissue/organs (spleen, kidney, liver, heart, lungs, sternum, muscle and bladder with urine) were collected and wet-weighed. Radioactivity associated with each tissue was assessed in a gamma-counter with internal standards (5 and 10 μl of the injected solution). Measurements were expressed as percentage of the injected dose per unit mass of organ (%ID/g) and were corrected for radioactivity decay, allowing the direct comparison of organs or animals.
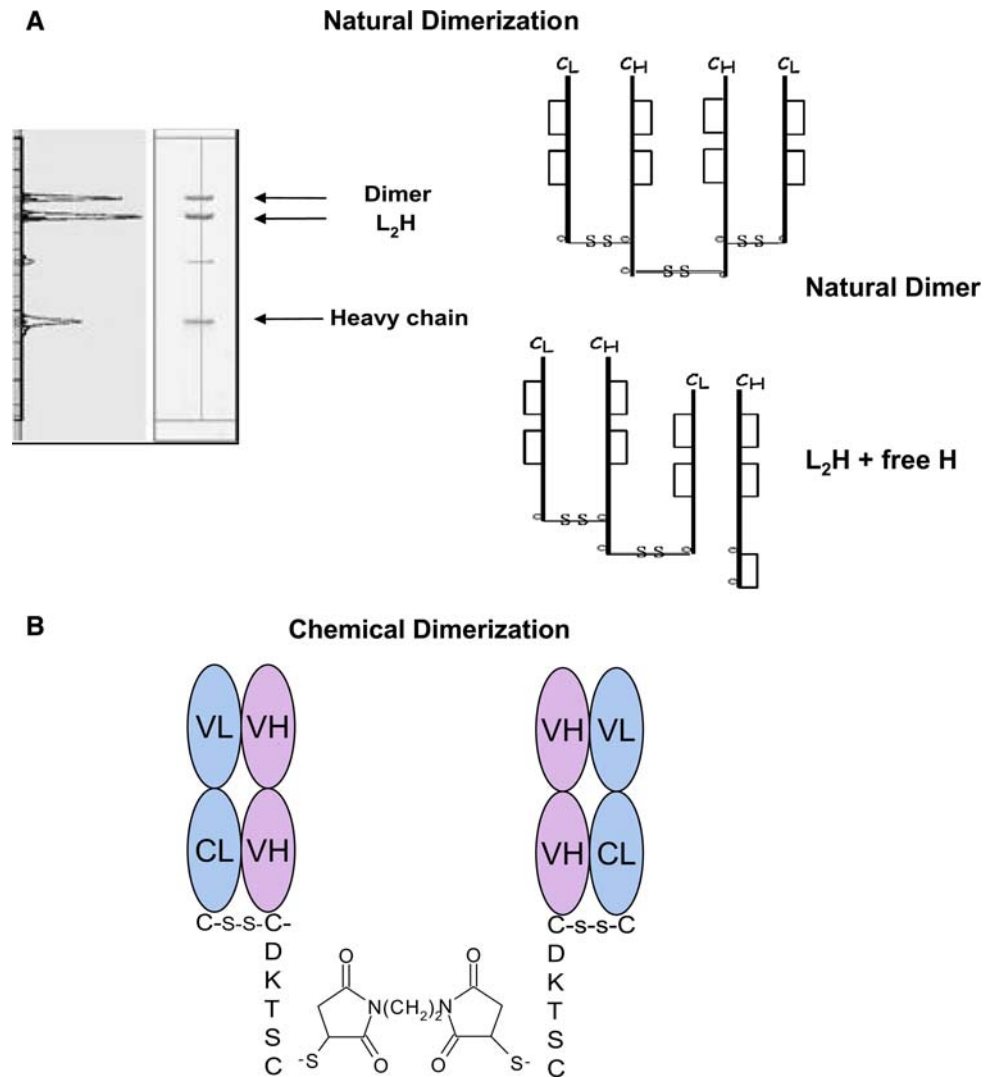
Results

C4 dimer generation

C4, a previously selected human antibody fragment, mimicking the specificity of MOV19 and characterized by a human lambda light chain, was selected as a potential candidate for further clinical exploitation on the basis of its binding kinetics and the molecule was engineered to a dimer format by genetic and chemical modification of the molecule. The N-terminal residue of heavy chains was a glutamine, which we converted to an asparagine to avoid the intramolecular cyclization reaction typically underwent by N-terminal glutamine residues [2]. Further, the addition of the penta-peptide DKTSC to the C-terminus of the heavy chain gave rise to a fragment with an extra free C-terminal cysteine residue corresponding to the first cysteine of the natural full-length antibody hinge region. After these modifications, C4 was renamed AFRA4.

The oxidation of the free cysteine residue enabled the formation of an $F(ab')_2$ natural dimer; SDS-PAGE analysis however revealed that the natural $F(ab')_2$ dimeric preparation was not homogeneous.

Several unexpected species were detectable by SDS-PAGE analysis, the most abundant one with an apparent molecular weight of 75 kDa (Fig. 1a). This species was found to result from the formation of a disulfide bridge between the C-terminal cysteine from one monomer and

the C-terminal cysteine of the light chain of a second *Fab* molecule. The resulting molecule was therefore composed by a monomer covalently linked to an extra light chain (L_2H) which is hydrophobically associated to a free heavy chain to form second *Fab* molecule. L_2H species represented 43% of the total protein.

Due to the heterogeneity in the natural dimer formation, this approach resulted not practicable; then, chemical dimerization was attempted using the linker BMOE that should generate a di-*Fab*-maleimide, DFM, by the formation of a thioether bond between the maleimide group of the linker and the unique free cysteine at the C-terminus of the AFRA4 heavy chain (Fig. 1b). However, extremely poor yields of AFRA-DFM 4 were obtained by chemical dimerization and, after complete reduction of the "natural" dimer, only 4% of DFM was recovered. Despite repeated attempts and optimization of the protocol, it was not possible to gain significant improvement in the reaction yield.

Generation of new human anti-FR antibody (AFRA) fragments

To obtain new antibody fragments directed against FR, we constructed human antibody libraries starting from the pool of RNA extracted from the PBMC of four selected EOC patients (EOC pts' Libraries). Using a wide panel of primers to rescue the maximum variability (see V-base website for sequences), we amplified 4 different libraries: VHCH1 from IgM, VHCH1 from IgG, VλCλ and VκCκ (size 7.5×10^6, 7.6×10^6, 2×10^6 and 1.6×10^6, respectively). Sequencing of 50 randomly selected clones to assess the variability of each library revealed no identical sequences (data not shown).

To search for human antibody fragments sharing the same specificity for FR as our murine mAbs we used a guided selection procedure based essentially on three different steps: (1) selection of a human VHCH1 guided by the murine light chain; (2) cloning of the selected human

VHCH1 into a vector containing the human light chain libraries; and (3) selection of the human light chain guided by the previously isolated human VHCH1.

To generate human antibodies mimicking the specificity of MOV18 and MOV19, which are directed against two non-overlapping epitopes of the FR, we used: the light chain of MOV18 as a guiding template to select the human VHCH1 from the EOC pts' VHCH1 Library (pool of VHCH1 from IgM and from IgG); the human VHCH1 of C4 to select an antibody from the EOC pts' VκCκ Library in the attempt to obtain an antibody with more desirable characteristics than C4/AFRA4 concerning dimerization. Figure 2 shows the flow chart of the selection procedure.

The VκCκ of MOV18 was cloned (Fig. 2a), sequenced and used to guide the selection. The guided pairing was positively selected on A431FR cells instead of the OVCAR 3 cells used in selecting C4 [19], and negatively selected on the isogenic A431Mock cell line (Fig. 2b). After three rounds of selection, analysis by phage-ELISA identified eight VHCH1 able to bind A431FR but not A431Mock when paired with the MOV18 light chain. The binding specificity of the hybrid antibody was evaluated by immunofluorescence and/or ELISA on A431FR versus A431Mock cells. Sequencing revealed an identical sequence in all clones (data not shown).

The "MOV18 mimicking" huVHCH1 was paired with the EOC pts' lambda and kappa light chain libraries and panned on A431FR cells, while the "MOV19 mimicking" huVHCH1 of the C4 antibody was paired with the EOC pts' kappa light chain library and panned on OVCAR3 cells (Fig. 2c). After four and three rounds of panning for "MOV18 mimicking" and "MOV19 mimicking" human light chain selections, respectively, several phages were picked up randomly. Screening by monoclonal ELISA identified 21 clones that bound differentially to A431FR versus A431Mock cells. Sequencing of light chains of clones showing the highest binding identified three different light chains paired with the "MOV18 mimicking" huVHCH1 and one with the human "C4-MOV19 mimicking" huVHCH1. These fully human *Fab* fragments were respectively named AFRA1, -2 and -3 and AFRA5.

Our protocol using the C4 heavy chain as a guiding template resulted in the same heavy chain in both C4 and AFRA5. Thus the same N-terminal and C-terminal molecular modification were applied to AFRA5 that was then named AFRA5.3.

Characterization of AFRA fragment binding activity

The his-tag inserted in the sequence of the human *Fab*s allowed their purification at laboratory scale and, in turn, FACS analysis of their binding activity. Since AFRA5.3 was obtained by light chain reshuffling starting from the C4/AFRA4 binding specificity, the latter antibody fragment was included in the analysis to enable a more precise comparison. Table 1 summarizes the results obtained on a panel of ovarian carcinoma cell lines naturally expressing different FR levels and on the pair of isogenic lines differing only in the ectopic expression (A431FR) or absence of expression (A431Mock) of FR. All the reagents were specific since their binding to the non-FR-expressing cell lines A431Mock (see Table 1) and Mewo (data not shown) was at background level ($<20 \times 10^3$ total immunofluorescence). Among the cell lines with higher FR overexpression, and consistent with the total binding of the guiding original reagent (data not shown), reactivity of AFRA1, -2 and -3, "potentially mimicking MOV18", with A431FR cells was greater than that with OVCAR3 cells, while AFRA4 and AFRA5.3 "potentially mimicking MOV19" equally bound these lines. Only human *Fab*s AFRA1 and AFRA5.3 recognized FR when it was expressed at low levels in OAW42, OVCA432 and SKOV3 ovarian cancer cells. AFRA5.3, as the highest binder, was selected for further characterization with respect to its potential application upon dimerization.

AFRA5.3 dimer generation

AFRA5.3 was purified to homogeneity and its binding kinetics was initially compared to that of AFRA4 by surface plasmon resonance. The respective binding affinities
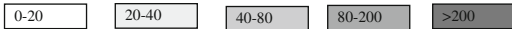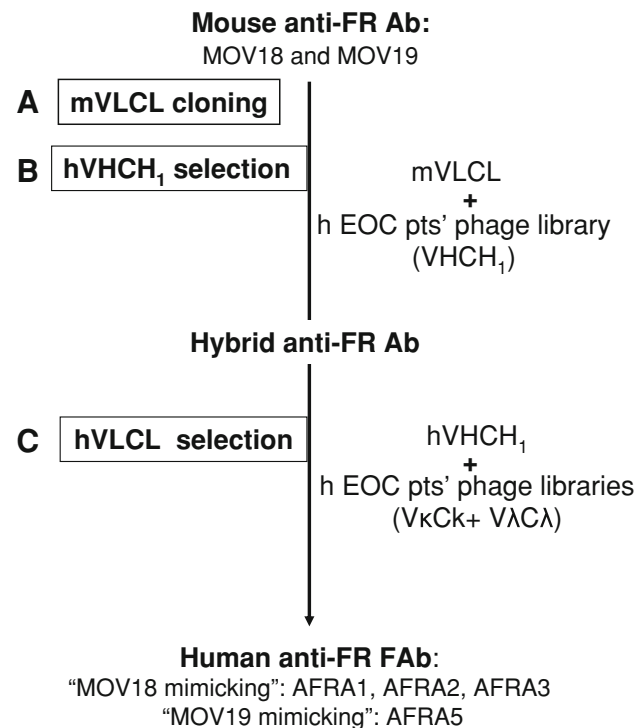
Mouse anti-FR Ab:
MOV18 and MOV19

A | mVLCL cloning |

B | hVHCH₁ selection | mVLCL
                            +
                   h EOC pts' phage library
                            (VHCH₁)

Hybrid anti-FR Ab

C | hVLCL selection | hVHCH₁
                            +
                   h EOC pts' phage libraries
                        (VκCk+ VλCλ)

Human anti-FR FAb:
"MOV18 mimicking": AFRA1, AFRA2, AFRA3
"MOV19 mimicking": AFRA5

Fig. 2 Flow chart of the strategy used to select the new human anti-FR *Fab* AFRA. *m* murine; *hu* human; *EOC pts' L* epithelial ovarian cancer patients' antibody libraries

Table 1 Binding activity in FACS analysis of selected anti-FR *Fab* fragments on cell lines naturally or ectopically expressing different levels of FR

| Antibody fragments | Binding activity on [a] | | | | | | |
| | EOC cell lines naturally expressing FR | | | | | Isogenic lines differing in FR | |
	OVCAR3 (3+)[b]	IGROV1 (2+)	OAW42 (1+)	OVCA432 (1+)	SKOv3 (1+)	A431FR (4+)	A431Mock (neg)
AFRA1	245	38	19	17	31	334	14
AFRA2	105	37	37	38	58	152	12
AFRA3	76	19	8	11	13	204	11
AFRA4	271	66	14	28	13	153	15
AFRA5.3	230	84	27	47	42	268	12

[a] The reported values are the mean total immunofluorescence binding $\times 10^{-3}$ obtained in 2–6 independent experiments; the binding values were also ranked in an arbitrary gray scale shadin: 0-20 20-40 40-80 80-200 >200

[b] The level of FR expression, as assessed by Western Blot analysis with a mixture of murine MOV18 and MOV19 antibodies, is reported in brackets in an arbitrary scale

deduced from the binding curves (Fig. 3a) showed that while both *Fab* fragments bound the immobilized antigen, AFRA5.3 had a higher association rate but also a faster dissociation. The calculated K_D (43.9 nM) of AFRA 5.3 was more than threefold lower than that of AFRA 4 (168 nM).

AFRA5.3 dimerization, expected to slow its dissociation rate and to further increase its avidity, was then attempted. The oxidation of the free cysteine residue of the AFRA5.3 heavy chain enabled the formation of a natural AFRA-$F(ab')_2$ 5.3; in this case, at variance from AFRA4, SDS-PAGE analysis revealed a higher degree of homogeneity. Indeed, L_2H species accounted for less than 16% of the total protein in preparations of AFRA-$F(ab')_2$ 5.3 (data not shown). Again at variance from AFRA4, chemical dimerization was successfully performed starting from AFRA5.3 and the overall percent of DFM obtained at the end of the reaction was at least 10-fold higher for AFRA-DFM5.3 (45%) than for AFRA-DFM4 (4%).

AFRA-DFM5.3 can be obtained at >90% purity, as assessed by SDS-PAGE analysis in reducing conditions (Fig. 4a) and by RP-HPLC (Fig. 4b), and the L_2H impurity accounted for <10% of the total protein. AFRA-DFM5.3, due to the strong hydrophobic association between L_2H and a free H chain, was resolved as a unique peak by gel filtration in physiologic conditions (data not shown). AFRA-DFM5.3 production and purification were scaled-up and produced in clinical grade conditions in the perspective of its future in vivo use.

AFRA-DFM5.3 binding activity in vitro and in situ

ELISA analysis of the AFRA-DFM5.3 dimer for reactivity with cell lines naturally or ectopically expressing FR showed that the dimer compared to the monomeric AFRA5.3 exhibited not only a higher binding but also the

typical binding curve of a bivalent molecule which reaches the plateau when the antibody is used in excess compared to the antigen. Figure 3b shows representative examples of the titration binding curves with IGROV1 cells, which naturally express FR at intermediate levels, and to A431FR cells, which ectopically express high levels of FR. BIAcore analysis confirmed the improvement of overall affinity in the dimer format and revealed that the improved binding capacity was due to slowing of the dissociation rate (Fig. 3c).

Immunohistochemical analysis of AFRA-DFM5.3 for its ability to recognize in situ the FR expressed on tumor surgical specimens showed that the dimer, as compared to murine MOV19 used to guide its selection, reacted only with the tumor areas and did not stain any surrounding healthy tissue (Fig. 5 shows a representative example of the four analyzed), confirming the specificity of AFRA-DFM5.3 in an in vivo context.

AFRA-DFM5.3 radiolabeling

To formally prove that AFRA-DFM5.3 mimics MOV19 binding, we conducted a competition assay using ^{131}I-AFRA-DFM5.3 in which this reagent specifically competed in both naturally and ectopically FR-expressing cell lines with the chimeric version of the anti-FR mAb used to guide its selection as entire molecule, chiMOV19, and as $(Fab')_2$ (Fig. 6a). Based on the slopes of the competition curves and the IC50 values, AFRA-DFM5.3 and chiMOV19 clearly recognize the same or overlapping epitopes. Furthermore, in agreement with previous data [9], AFRA-DFM5.3, as MOV19, induce an evident increment of chiMOV18 binding.

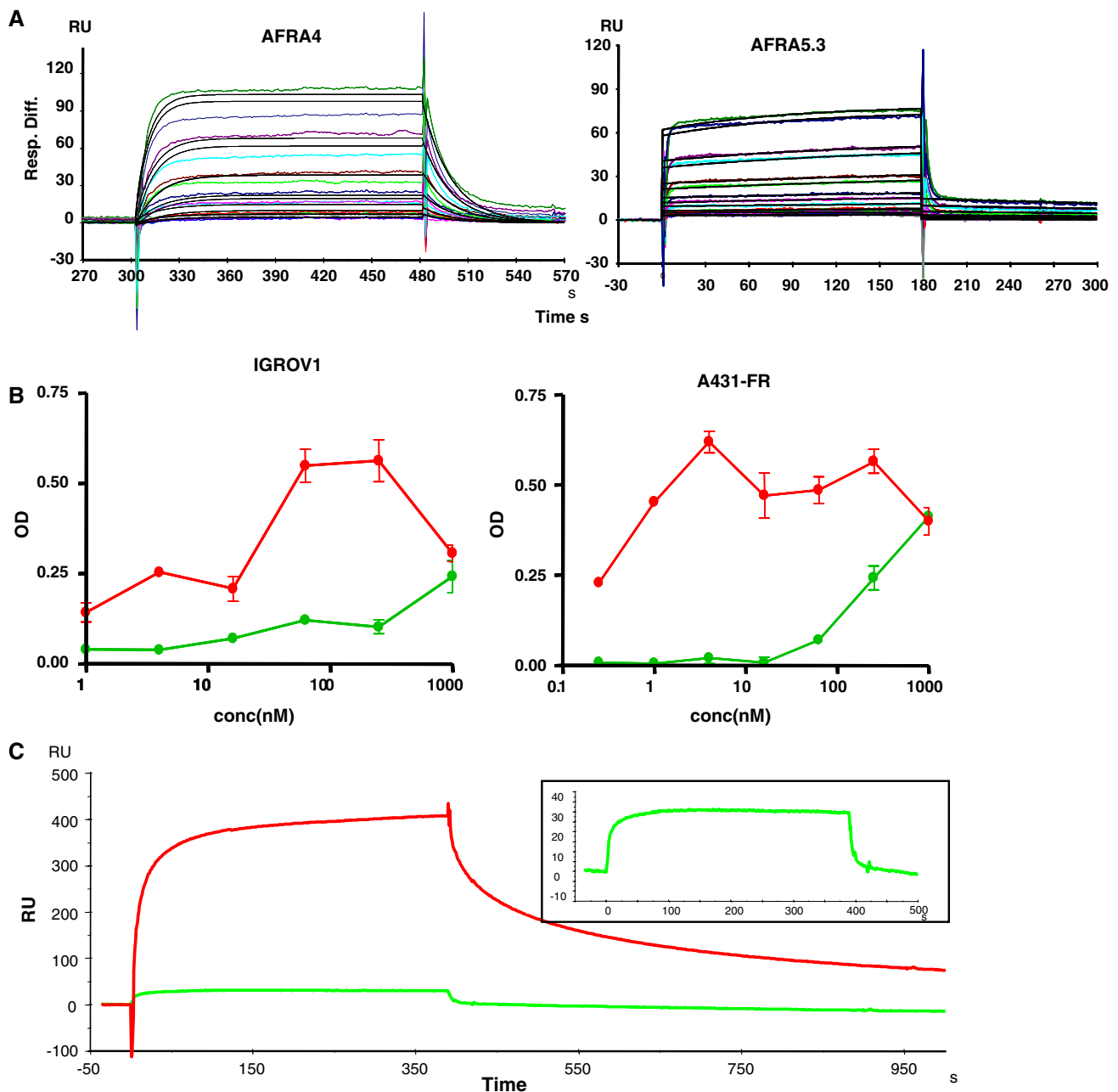Use of the Chizzonite method of radiolabeling preserved the integrity and functionality of AFRA-DFM5.3, with the

Fig. 3 BIAcore analysis. **a** Determination of human *Fab* binding parameters by surface plasmon resonance with BIAcore. Several concentrations of *Fab* monomer (3–200 nM) were applied on the sensor chip cell precoated with FR (280 RU). Binding was registered for 30 min and washes were monitored for another 20 min. *Left panel* AFRA5.3 binding curves ($K_D = 43.9$ nM, $\chi^2 = 1.85$); *Right panel* AFRA4 binding curves ($K_D = 168$ nM, $\chi^2 = 2.19$). **b** Titration binding activity of AFRA-DFM5.3 (dimer, *red lines*) as compared to AFRA5.3 (monomer, *green lines*) as evaluated by ELISA. **c** Comparison of binding and dissociation of AFRA-DFM5.3 (dimer, *red line*) and AFRA5.3 (monomer, *green line*) as evaluate by BIAcore analysis obtained at an injected concentration of 100 nM. To better appreciate the binding and dissociation of the monomer, the curve is amplified in the inset

final radiolabeled product at a specific activity of 196.1 ± 25.9 MBq/mg (mean $\pm$ SD, four experiments) and showing $68 \pm 5.2\%$ immunoreactivity (mean $\pm$ SD, four experiments). Analysis of ^{131}I-AFRA-DFM5.3 in vitro stability revealed no difference in functionality when kept for 24 h at 37 or 4°C in buffer or human serum, as evaluated by

direct binding on fixed cells (Fig. 6b, right panel), or in integrity, as assessed by SDS-PAGE (Fig. 6b, left panel). Furthermore, ^{131}I-AFRA-DFM5.3 injected into mice as a radiotracer maintained functionality (Fig. 6c, right panel) and integrity (Fig. 6c, left panel) in mouse sera until 3 h after the injection, as assessed by ELISA and SDS-PAGE,
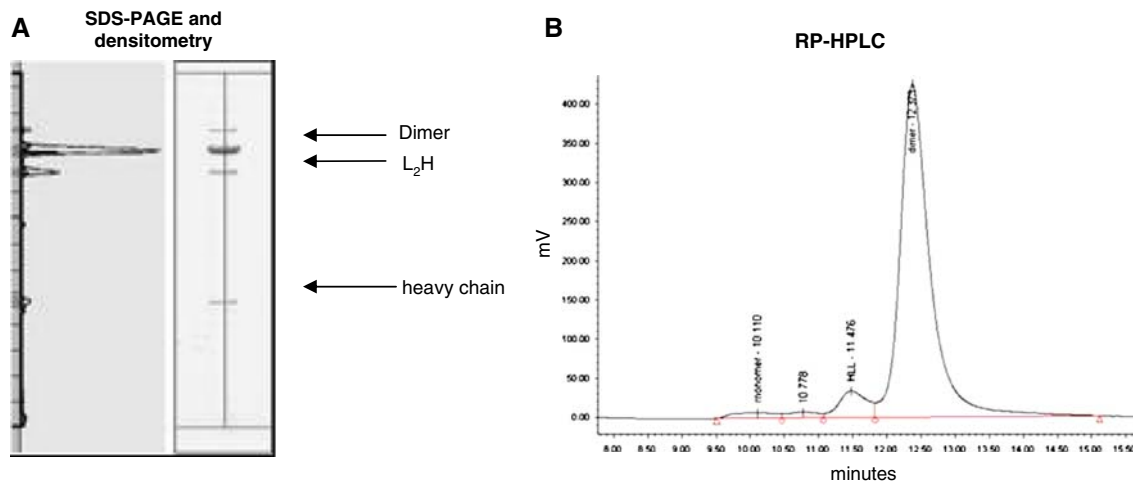
Fig. 4 AFRA-DFM5.3 purity. **a** SDS-PAGE (12.5%) analysis in non-reducing conditions; the relative densitometric results are reported at the left of the slab. **b** RP-HPLC analysis. In both analyzes the molecular species were identified based on the relative molecular weight as dimer, L_2H and free H chain

Fig. 5 AFRA-DFM5.3 in situ binding activity. Immunohistochemistry on serial cryostat sections from a serous ovarian carcinoma with AFRA-DFM5.3 and murine MOV19
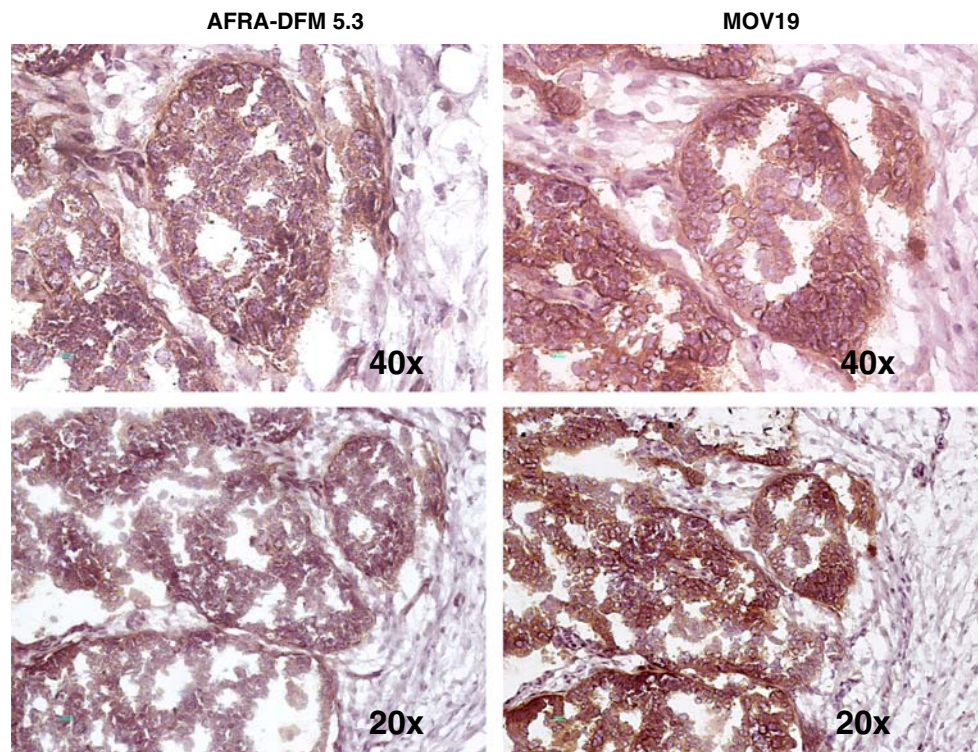
respectively, showing a pattern of results comparable to that of the ^{131}I-AFRA-DFM5.3 before in vivo injection.

Preclinical in vivo characterization

A preliminary localization experiment was carried out in mice injected s.c. with A431FR or the FR-non-expressing isogenic A431Mock cells followed by injection of AFRA-DFM5.3. Tumors were collected 12 or 24 h later for immunohistochemical processing. The presence of AFRA-DFM5.3 in the tumor masses, as detected by direct incubation of the tumor cryosections with an anti-human *Fab* peroxidase, was evident at 24 h after injection only in FR-expressing tumors (representative examples in Fig. 7a). Consistent with localization data obtained with unlabeled AFRA-DFM5.3, ^{131}I-AFRA-DFM5.3 showed different elimination curves for blood and for tumors (Fig. 7b shows data from a representative experiment of three performed). Blood clearance and blood terminal half-life ($t_{1/2}\beta$) were similar in the A431FR- and A431Mock-bearing mice (mean ± SD: 3.72 ± 0.09 and 3.64 ± 0.15, respectively), and shorter than those in the tumors, where ^{131}I-AFRA-DFM5.3
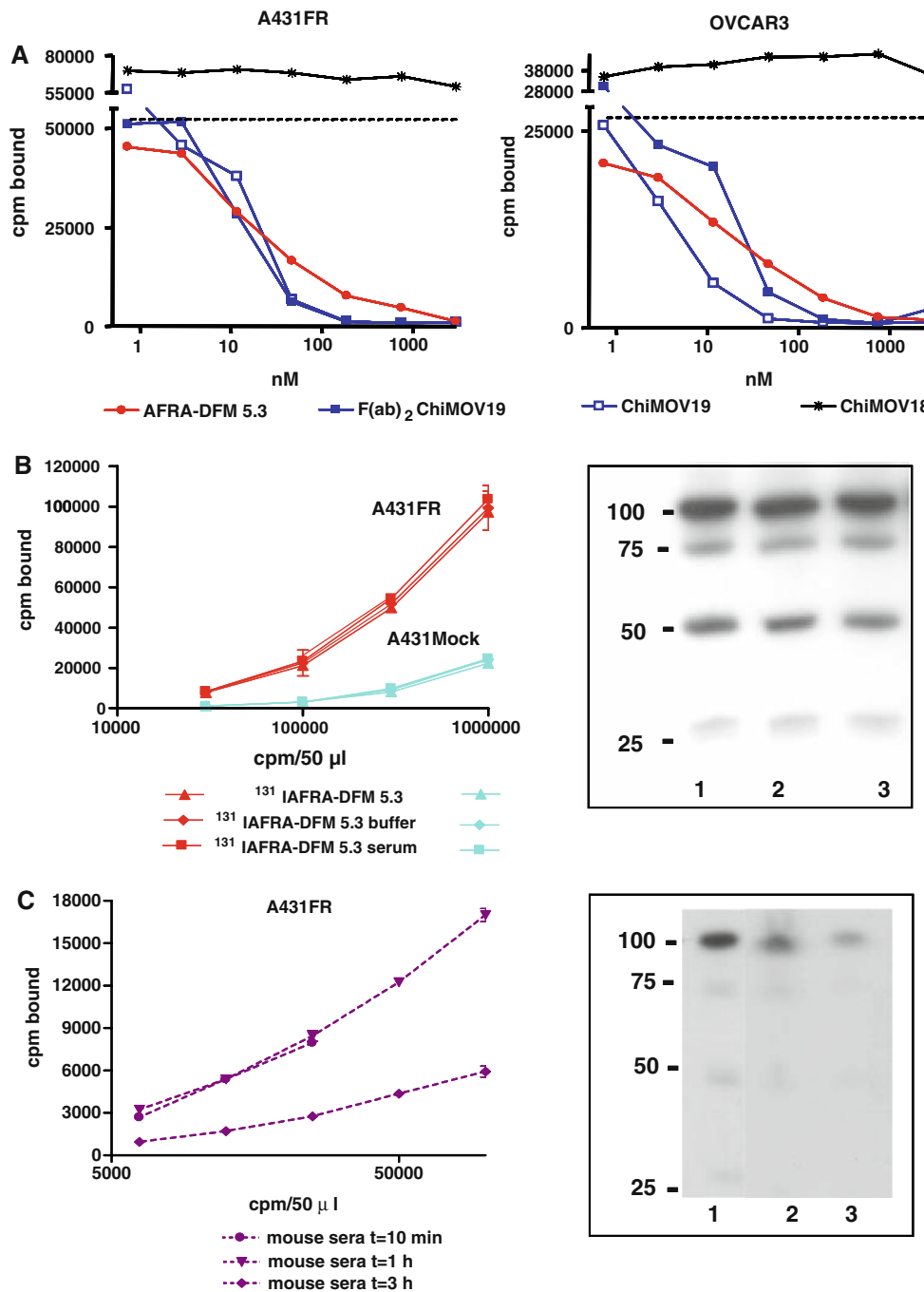
Fig. 6 Characterization of the ^{131}I-labeled AFRA-DFM5.3. **a** Competition of ^{131}I-AFRA-DFM5.3 binding on FR-expressing cells. IC_{50} extrapolated from titration curves were: on A431FR cells, AFRA-DFM5.3 = 15.3 nM, chiMOV18 = not applicable, chiMOV19 = 20.2 nM and $(Fab)_2$-chiMOV19 = 13.8 nM; on OVCAR3 cells, AFRA-DFM5.3 = 11.6 nM, chiMOV18 = not applicable, chiMOV19 = 4.1 nM and $(Fab)_2$-chiMOV19 = 21.2 nM. **b** *Left panel* direct binding activity of ^{131}I-AFRA-DFM5.3 following incubation for 24 h at 37°C in buffer or serum as compared to that of the labeled reagent incubated in buffer at 4°C, as evaluated on FR-expressing (A431FR) or non-expressing (A431Mock) cells. *Right panel* analysis of ^{131}I-AFRA-DFM5.3 integ-rity by autoradiography of samples run in SDS-PAGE (12.5%) in non-reducing conditions. *Lane 1* = ^{131}I-AFRA-DFM5.3 24 h at 4°C in buffer; *lanes 2* and *3* = ^{131}I-AFRA-DFM5.3 24 h at 37°C in buffer or human serum, respectively. **c** *Left panel* direct binding activity of mouse sera collected 10 min, 1 h and 3 h after ^{131}I-AFRA-DFM5.3 i.v. injection. *Right panel* analysis of ^{131}I-AFRA-DFM5.3 integrity by autoradiography of samples run in SDS-PAGE (12.5%) in non-reducing conditions. *Lane 1* = ^{131}I-AFRA-DFM5.3 in buffer; *lanes 2* and *3* = sera of mice 30 min and 1 h, respectively, after ^{131}I-AFRA-DFM5.3 i.v. injection. Longer exposure of the gel revealed similar band patterns in sera at 3 h after injection (data not shown)
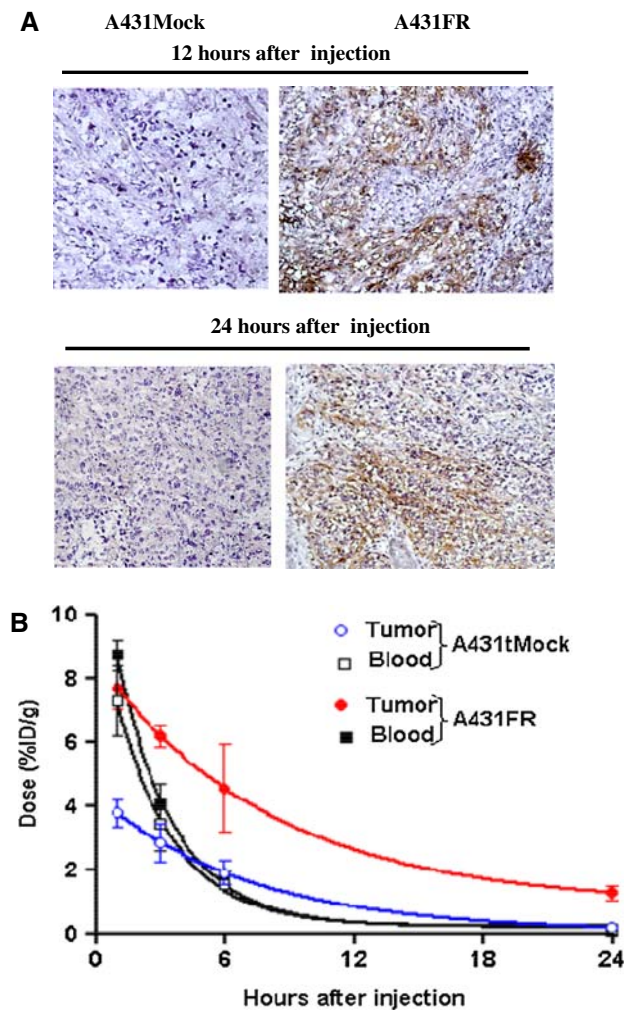
Fig. 7 AFRA-DFM5.3 in vivo preclinical activity. **a** Ex vivo localization of AFRA-DFM5.3 in s.c.-growing A431FR and A431Mock tumors. The i.v. administration of DFM-AFRA5.3 (200 µg/mouse) was followed by tumor explant after 12 h or 24 h. Cryosections were directly immunoreacted with anti-hu *Fab* peroxidase. **b** In vivo localization of ^{131}I-AFRA-DFM5.3 (1–1.5 MBq/mouse) following i.v administration. The pharmacokinetics was evaluated in the blood and tumor of mice injected s.c. with A431FR or A431Mock cells. Values are expressed as mean % injected dose/g $\pm$ SE in groups of 3–4 mice for each time point in a representative experiment of three performed

concentrations at 3 h post-injection in A431FR tumors began to exceed those measured in blood. At 3 h in the three experiments, the mean %ID/g was 6.29 ± 0.16 and 2.84 ± 1.04 and tumor/blood ratio 1.23 and 0.83 in A431FR and A431Mock tumors, respectively. Despite rapid blood clearance, ^{131}I-AFRA-DFM5.3 remained for a longer time in FR-expressing tumors than in control tumors (tumor/blood ratio at 24 h: 9.09 and 1.41, respectively). The biodistribution of 131-AFRA-DFM5.3 in tissues/organs other than the tumor was comparable in A431FR- and A431Mock-bearing mice, and elevated values corresponding to bladder and urine correlated well with the

expected dimer excretion through a functional detoxification pathway. To enable evaluation of inter-assay variability, Table 2 gives the results of ^{131}I-AFRA-DFM5.3 biodistribution as %ID/g and tissue/organs:blood ratio as a mean of the three experiments performed.

Discussion

Although a number of technologies, such as phage display and ribosome display, are presently available for generation of completely human antibodies [7], some relevant limitations in raising new human antibodies have been identified. In particular, antibodies isolated from nonimmune libraries often exhibit binding affinities not adequate for in vivo use, and phage selection, while very effective with purified antigen, is more difficult with complex mixtures of antigens, such as cell surface antigens which differ widely in type and expression levels. Phage antibodies have been derived by selection on cells [24], such as hematopoietic [26] and melanoma cells [16] and have been used successfully. Unfortunately, the method utilized for cell-based panning typically yield a panel of single-chain Fv (scFv) molecules that are specific for dominant or abundant surface antigens, often obscuring the desired clones. Guided selection method enables the humanization of murine antibody and gives the possibility to raise antibody against a specific epitope remarkably reducing the selection of unwanted phages. Using this method, we had a successful tumor cell-based selection of the human anti-FR fragment C4 [19] of potential clinical utility.

To exploit the specificity and affinity of C4 reagent, we attempted to generate natural and chemical dimers by its genetic and chemical modifications, respectively. After N-terminal site directed mutagenesis and adding the natural hinge sequence of the gamma 1 human family to the C-terminus of the heavy chain, natural dimers were easily obtained with AFRA4, but AFRA4-$F(ab')_2$ preparations presented an unexpectedly high amount of aberrant L_2H species that in physiologic condition associated with free H chain. Even non-covalently bound, this anomalous Fab_2 form was found to be very stable, as demonstrated by resolution in a single peak in gel filtration, in agreement with literature data [20, 35]. The unusual reactivity of AFRA4 in the natural dimerization process was even more pronounced in the chemical dimerization; less than 5% of the AFRA4 molecules reacted with the linker, and step-by-step monitoring of DFM formation using mass spectrometry revealed no further reactivity with further excess of the maleimido reactant. C4/AFRA4 antibody fragment, isolated from naïve dual combinatorial libraries, is characterized by a lambda light chain. Although Vλ genes encode 30–40% of light chains in the Ig repertoire of healthy

Table 2 Biodistribution and tumor uptake of ^{131}I-AFRA-DFM5.3, expressed as %ID/g and tissue/organ: blood ratio (T/B), following i.v. administration in athymic mice

Tissue/organ	A431FR-bearing mice			A431Mock-bearing mice		
	%ID/g		T/B	%ID/g		T/B
	Mean	SD		Mean	SD	
1 h after injection						
Blood	12.37	3.17	1.00	7.27	1.88	1.00
Tumor	**5.35**	**2.07**	**0.43**	**3.77**	**0.75**	**0.52**
Spleen	4.99	1.25	0.40	4.01	0.37	0.55
Kidney	30.95	4.68	2.50	30.67	4.94	4.22
Liver	6.31	2.64	0.51	3.43	0.71	0.47
Heart	4.56	1.34	0.37	3.04	0.36	0.42
Lungs	4.95	0.83	0.40	3.99	0.13	0.55
Sternum	1.81	0.23	0.15	1.33	0.09	0.18
Muscle	1.08	0.12	0.09	1.03	0.11	0.14
Urine + bladder	56.87	27.11	4.60	87.45	20.86	12.03
3 h after injection						
Blood	5.11	1.53	1.00	3.41	1.42	1.00
Tumor	**6.29**	**0.16**	**1.23**	**2.84**	**1.04**	**0.83**
Spleen	2.89	1.01	0.57	1.90	0.76	0.56
Kidney	12.69	9.85	2.48	4.01	1.01	1.18
Liver	3.07	1.76	0.60	1.44	0.64	0.42
Heart	2.00	0.75	0.39	1.42	0.47	0.42
Lungs	6.98	6.13	1.36	2.57	1.10	0.75
Sternum	1.19	0.21	0.23	0.84	0.28	0.25
Muscle	0.93	0.17	0.18	0.69	0.37	0.20
Urine + bladder	151.51	84.38	29.65	99.73	11.87	29.24
6 h after injection						
Blood	2.10	0.50	1.00	1.53	0.02	1.00
Tumor	**4.56**	**0.01**	**2.17**	**1.89**	**0.64**	**1.23**
Spleen	1.67	1.18	0.80	1.34	0.68	0.88
Kidney	3.54	1.77	1.69	2.18	0.35	1.43
Liver	1.13	0.57	0.54	0.72	0.12	0.47
Heart	0.84	0.38	0.40	0.69	0.15	0.45
Lungs	1.68	0.64	0.80	1.41	0.13	0.92
Sternum	0.63	0.40	0.30	0.40	0.06	0.26
Muscle	0.39	0.03	0.19	0.36	0.08	0.23
Urine + bladder	94.55	76.63	45.03	72.72	41.07	47.53
24 h after injection						
Blood	0.20	0.13	1.00	0.13	0.02	1.00
Tumor	**1.77**	**0.47**	**9.09**	**0.18**	**0.05**	**1.41**
Spleen	0.23	0.17	1.16	0.14	0.02	1.14
Kidney	0.46	0.30	2.36	0.32	0.01	2.53
Liver	0.23	0.19	1.20	0.13	0.01	1.05
Heart	0.10	0.06	0.49	0.06	0.01	0.44
Lungs	0.29	0.10	1.49	0.13	0.04	1.05
Sternum	0.10	0.10	0.51	0.03	0.00	0.23
Muscle	0.05	0.01	0.26	0.04	0.03	0.32
Urine + bladder	14.42	8.63	73.95	1.08	0.38	8.61

subjects, a very limited number of anti-cancer human reagents with lambda pairing have been reported. We have also observed that this particular lambda chain has a high tendency to form homodimers that could affect the microorganism metabolism and final process yield. Further studies are needed to determine whether conformational characteristics of the AFRA4 lambda light chain play a role in the unusual chemical dimer formation.

Therefore, we decided to use guided selection and chain shuffling to generate new and diverse repertoires of human antibody fragments directed against FR, a target antigen of proven clinical utility for EOC treatment. Our initial step in the generation of new anti-FR human antibodies was the design, construction and characterization of a large *Fab* dual combinatorial human antibody phage display library derived from the rearranged V-genes of lymphocytes from patients with a previous history of EOC. Accumulating evidence indicates the presence of antibodies against several tumor-associated antigens (TAAs) in cancer sera and the association between these antibody levels and better prognosis and longer survival [5, 14, 36]. Although we did not specifically analyze and select the EOC donors of PBMC, used for library generation, for the presence of an antibody response against our target of interest, i.e. FR, elevated levels of anti-FR antibodies coupled with the presence of both CD4 and CD8 T-cell immunity have been reported in ovary and breast cancer patients, indicating that FR can elicit a coordinated immune response in cancer patients [22]. Thus, our choice of EOC patients (patients with a previous history of advanced-stage disease but tumor-free for more than 1 year at the time of blood withdrawal) argues for an in vivo-matured antibody repertoire potentially containing anti-TAAs and anti-FR antibodies. Furthermore, the wide array of primers used for primary amplification of human antibody variable domains [19] and the size of the heavy and light chain libraries ($\sim$7.5 $\times$ 10^6 VHCH1 from IgM, 7.6 $\times$ 10^6 VHCH1 from IgG, 2 $\times$ 10^6 VλCλ and 1.6 $\times$ 10^6 VKCK) could give raise to a large combinatorial library (potentially 10^{12} diverse combinations), suggesting the adequacy of these EOC libraries for our aim and their future usefulness for generation of other anti-TAA antibodies.

As a second step, we combined these "immune" libraries with epitope imprinting selection [18], a method that permits isolation of an antibody with the same specificity as a preexisting antibody by guided selection. Because the selection of antibodies against proteins expressed in their native conformation on the surface of tumor cells is frequently hampered by the relatively low abundance of the target antigen of interest as compared to the vast variety of other cell surface proteins, the guided pairing against FR was initially selected on the FR-ectopically expressing

A431FR cells instead of the FR-naturally expressing OVCAR3 cells used to select C4 [19]. The potential advantages of A431FR cells are the extremely high overexpression of the target antigen and the possibility of negative selection on the isogenic A431Mock cells [11]. In parallel, we proceeded with light chain reshuffling to combine the human heavy chain of C4 with the EOC pts' kappa light chain library, and with panning on OVCAR3 cells. These approaches enabled the generation of four new and completely human anti-FR reagents.

Selection of the best candidate for subsequent clinical application among the four new available anti-FR human *Fab* fragments was initially based on flow cytometry analysis of a panel of cell lines expressing FR at different levels. This analysis revealed that all the new reagents, regardless of the origin of the cells used for panning, exhibited a clear binding to cells naturally expressing the target antigen at high levels; however, a preferential recognition of the cells guiding selection was also observed. Although further studies on the fine specificity of each selected *Fab* are needed to draw clear conclusions, these data suggest that cell-based selection approaches should also consider the cellular context in which the antigen is expressed since this might affect antigen molecular conformation and ultimately the antigen–antibody interaction. The initial flow cytometric screening of all selected *Fab* fragments suggested that they exhibited a binding affinity in the two-digit nanomolar range, supporting our hypothesis that our libraries are potentially biased toward an anti-tumor and anti-FR response.

Recognition of antigen in its native state implies a greater likelihood that the antibody will retain reactivity during in vivo applications. Accordingly, we selected the new AFRA5 human *Fab* as the best candidate for further characterization studies and its sequence was optimized upon genetic modification at N- and C-termini as previously performed starting from the original *Fab* fragment C4.

BIAcore evaluation of AFRA5.3 confirmed a binding affinity (K_D = 44 nM) in the nanomolar range and indicated a higher association but also a faster dissociation rate for AFRA5.3 as compared to AFRA4. This latter binding kinetics might be disadvantageous for an antibody used in vivo for therapeutic application such as radioimmunotherapy, since once the antibody binds to the tumor, continued occupation of the binding site is essential for efficient radiation delivery.

Dimerization could overcome this limitation and, unlike the very low yield of AFRA-DFM 4 formation, AFRA-DFM5.3 was obtained at high yield and at a final purity compatible with clinical development. BIAcore analysis confirmed that the overall affinity of AFRA-DFM5.3 in the chemical dimer format was improved and that a slower

dissociation rate accounts for the improved binding capacity. AFRA-DFM5.3 exhibited an overall binding affinity very similar to that of the anti-FR antibody MOV18 (data not shown) already entered in the clinics, further supporting its suitability for in vivo localization of ovarian cancer cells.

The AFRA-DFM molecule does not require glycosylation for binding activity as moiety targeting radioisotopes and is therefore compatible with microorganism production and the associated advantages for clinical production at high yield. Shifting the *Fab* to the chemical dimer format conferred the further advantage of increased overall binding strength, and the optimized AFRA-DFM5.3 reagent was validated for competition ability, recognition of the target antigen in clinical specimens, and in vitro and in vivo stability after radiolabeling. Preliminary evaluation of ^{131}I-AFRA-DFM5.3 at radiotracer doses in a well-defined pre-clinical animal model [11] indicated that the blood clearance and the tumor retention were in the range of those obtained with similar molecules in different experimental systems [4]. The observed pharmacokinetic parameters were compatible with the size and the human origin of the molecule, and the adequate and specific tumor localization supports a potential therapeutic use. Evaluation of the ability of ^{131}I-AFRA-DFM5.3 to control tumor growth when delivered at therapeutic doses is ongoing. Due to its binding specificity and short half-life, AFRA-DFM5.3, following radiolabelling with suitable radioisotopes as ^{99}Tc or ^{111}In, might be also used for diagnostic localization of EOC metastatic deposits.

Finally, because phage antibody can be routinely converted into various forms, including full-length IgG molecule, without loss of pre-selected specificity and functionality [23], other applications can also be envisaged for our anti-FR *Fab*s. In particular, the availability of antibody specificities directed to different non-overlapping epitopes of FR, such as those of AFRA1 and AFRA5.3, might serve to generate, in a mammalian expression system, properly glycosylated full-length IgG molecules suited for a strategy of treatment depending on entirely human anti-FR IgG antibodies for complement activation. In fact, our recent study using chimeric versions of MOV18 and MOV19 showed that effective complement activation was possible only when two spatially close epitopes of FR were simultaneously engaged by the mixture of the two antibodies in the presence of anti-mCRP reagents [25].

Overall, our studies demonstrate that the new antibody phage display libraries enables the selection of completely human *Fab*s directed against ovary carcinoma and that one of these *Fab*s, AFRA5.3, upon genetic and chemical manipulation, is suited for future clinical application in ovarian cancer.

References

1. Committee on cancer research (UKCCCR), United Kingdom (1998) Guidelines for the welfare of animals in experimental neoplasia, 2nd edn. Br J Cancer 77: 1–10

2. Adamczyk M, Gebler JC, Wu J, Yu Z (2002) Complete sequencing of anti-vancomycin *Fab* fragment by liquid chromatography-electrospray ion trap mass spectrometry with a combination of database searching and manual interpretation of the MS/MS spectra. J Immunol Methods 260:235–249

3. Alberti S, Miotti S, Fornaro M, Mantovani L, Walter S, Canevari S, Ménard S, Colnaghi MI (1990) The Ca-MOv18 molecule, a cell-surface marker of human ovarian carcinomas, is anchored to the cell membrane by phosphatidylinositol. Biochem Biophys Res Commun 171:1051–1055

4. Brack SS, Silacci M, Birchler M, Neri D (2006) Tumor-targeting properties of novel antibodies specific to the large isoform of tenascin-C. Clin Cancer Res 12:3200–3208

5. Canevari S, Pupa SM, Menard S (1996) 1975–1995 revised anti-cancer serological response: biological significance and clinical implications. Ann Oncol 7:227–232

6. Canevari S, Stoter G, Arienti F, Bolis G, Colnaghi MI, Di Re E, Eggermont AMM, Goey SH, Gratama JW, Lamers CHJ, Nooy MA, Parmiani G, Raspagliesi F, Ravagnani F, Scarfone G, Trimbos JB, Warnaar SO, Bolhuis RLH (1995) Regression of advanced ovarian carcinoma by intraperitoneal treatment with autologous T-lymphocytes retargeted by a bispecific monoclonal antibody. J Natl Cancer Inst 87:1463–1469

7. Carter PJ (2006) Potent antibody therapeutics by design. Nat Rev Immunol 6:343–357

8. Casalini P, Luison E, nard S, Colnaghi MI, Paganelli G, Canevari S (1997) Tumor pretargeting: role of avidin/streptavidin on monoclonal antibody internalization. J Nucl Med 38:1378–1381

9. Casalini P, Mezzanzanica D, Canevari S, Della Torre G, Miotti S, Colnaghi MI, Matzku S (1991) Use of combination of monoclonal antibodies directed against three distinct epitopes of a tumor-associated antigen: analysis of cell binding and internalization. Int J Cancer 48:284–290

10. Casey JL, King DJ, Chaplin LC, Haines AM, Pedley RB, Mountain A, Yarranton GT, Begent RH (1996) Preparation, characterisation and tumour targeting of cross-linked divalent and trivalent anti-tumour *Fab'* fragments. Br J Cancer 74:1397–1405

11. Coliva A, Zacchetti A, Luison E, Tomassetti A, Bongarzone I, Seregni E, Bombardieri E, Martin F, Giussani A, Figini M, Canevari S (2005) 90Y labeling of monoclonal antibody MOv18 and preclinical validation for radioimmunotherapy of human ovarian carcinomas. Cancer Immunol Immunother 54:1200–1213

12. Coney LR, Mezzanzanica D, Sanborn D, Casalini P, Colnaghi MI, Zurawski VR Jr (1994) Chimeric murine-human antibodies directed against folate binding receptor are efficient mediators of ovarian carcinoma cell killing. Cancer Res 54:2448–2455

13. Coney LR, Tomassetti A, Carayannopoulos L, Frasca V, Kamen BA, Colnaghi MI, Zurawski VR Jr (1991) Cloning of a tumor-associated antigen: MOv18 and MOv19 antibodies recognize a folate-binding protein. Cancer Res 51:6125–6132

14. Coronella-Wood JA, Hersh EM (2003) Naturally occurring B-cell responses to breast cancer. Cancer Immunol Immunother 52:715–738

15. Crippa F, Bolis G, Seregni E, Gavoni N, Bombardieri E, Scarfone G, Ferrari C, Buraggi GL (1995) Single dose intraperitoneal radio-

immunotherapy with the murine monoclonal antibody 131I-MOv18: clinical results in patients with minimal residual disease of ovarian cancer. Eur J Cancer 31A:686–690

16. de Kruif J, van der Vuurst de Vries AR, Cilenti L, Boel E, van Ewijk W, Logtenberg T (1996) New perspectives on recombinant human antibodies. Immunol Today 17:453–455

17. Figini M, Ferri R, Mezzanzanica D, Bagnoli M, Luison E, Miotti S, Canevari S (2003) Reversion of transformed phenotype in ovarian cancer cells by intracellular expression of anti-folate receptor antibodies. Gene Ther 10:1018–1025

18. Figini M, Marks JD, Winter G, Griffiths AD (1994) In vitro assembly of repertoires of antibody chains on the surface of phage by renaturation. J Mol Biol 239:68–78

19. Figini M, Obici L, Mezzanzanica D, Griffiths AD, Colnaghi MI, Winter G, Canevari S (1998) Panning phage antibody libraries on cells: isolation of human *Fab* fragments against ovarian carcinoma using guided selection. Cancer Res 58:991–996

20. Groulet A, Dorvillius M, Pelegrin A, Barbet J, Baty D (2002) Pharmacokinetic and tumor-seeking properties of recombinant and nonrecombinant anti-carcinoembryonic antigen antibody fragments. Int J Cancer 100:367–374

21. Jain M, Venkatraman G, Batra SK (2007) Optimization of radio-immunotherapy of solid tumors: biological impediments and their modulation. Clin Cancer Res 13:1374–1382

22. Knutson KL, Krco CJ, Erskine CL, Goodman K, Kelemen LE, Wettstein PJ, Low PS, Hartmann LC, Kalli KR (2006) T-cell immunity to the folate receptor alpha is prevalent in women with breast or ovarian cancer. J Clin Oncol 24:4254–4261

23. Liu B, Conrad F, Roth A, Drummond DC, Simko JP, Marks JD (2007) Recombinant full-length human IgG1s targeting hormone-refractory prostate cancer. J Mol Med 85:1113–1123

24. Loo L, Robinson MK, Adams GP (2008) Antibody engineering principles and applications. Cancer J 14(3):149–153

25. Macor P, Mezzanzanica D, Cossetti C, Alberti P, Figini M, Canevari S, Tedesco F (2006) Complement activated by chimeric anti-folate receptor antibodies is an efficient effector system to control ovarian carcinoma. Cancer Res 66:3876–3883

26. Marks JD, Ouwehand WH, Bye JM, Finnern R, Gorick BD, Voak D, Thorpe S, Hughes-Jones NC, Winter G (1993) Human antibody fragments specific for human blood group antigens from a phage display library. Biotechnology 11:1145–1149

27. Mayor S, Rothberg KG, Maxfield FR (1994) Sequestration of GPI-anchored proteins in caveolae triggered by cross-linking. Science 264:1948–1951

28. Meredith RF, Buchsbaum DJ, Alvarez RD, LoBuglio AF (2007) Brief overview of preclinical and clinical studies in the development of intraperitoneal radioimmunotherapy for ovarian cancer. Clin Cancer Res 13:5643s–5645s

29. Miotti S, Canevari S, Ménard S, Mezzanzanica D, Porro G, Pupa SM, Regazzoni M, Tagliabue E, Colnaghi MI (1987) Characterization of human ovarian carcinoma-associated antigens defined by novel monoclonal antibodies with tumor-restricted specificity. Int J Cancer 39:297–303

30. Miotti S, Negri DR, Valota O, Calabrese M, Bolhuis RL, Gratama JW, Colnaghi MI, Canevari S (1999) Level of anti-mouse antibody response induced by bispecific monoclonal antibody OC/TR in ovarian carcinoma patients is associated with longer survival. Int J Cancer 84:62–68

31. Mirick GR, Bradt BM, Denardo SJ, Denardo GL (2004) A review of human anti-globulin antibody (HAGA, HAMA, HACA, HAHA) responses to monoclonal antibodies. Not four letter words. Q J Nucl Med Mol Imaging 48:251–257

32. Ottone F, Miotti S, Bottini C, Bagnoli M, Perego P, Colnaghi MI, Ménard S (1997) Relationship between folate binding protein expression and cisplatin sensitivity in ovarian carcinoma cell lines. Br J Cancer 76:77–82

33. Presta LG (2006) Engineering of therapeutic antibodies to minimize immunogenicity and optimize function. Adv Drug Deliv Rev 58:640–656

34. Reichert JM, Valge-Archer VE (2007) Development trends for monoclonal antibody cancer therapeutics. Nat Rev Drug Discov 6:349–356

35. Rodrigues ML, Snedecor B, Chen C, Wong WL, Garg S, Blank GS, Maneval D, Carter P (1993) Engineering *Fab'* fragments for efficient *F(ab)*2 formation in *Escherichia coli* and for improved in vivo stability. J Immunol 151:6954–6961

36. Saif MW, Zalonis A, Syrigos K (2007) The clinical significance of autoantibodies in gastrointestinal malignancies: an overview. Expert Opin Biol Ther 7:493–507

37. Salazar MD, Ratnam M (2007) The folate receptor: what does it promise in tissue-targeted therapeutics? Cancer Metastasis Rev 26:141–152

38. Toffoli G, Cernigoi C, Russo A, Gallo A, Bagnoli M, Boiocchi M (1997) Overexpression of folate binding protein in ovarian cancers. Int J Cancer 74:193–198